# SURVEYOR TERMINAL GUIDANCE[1]

R. K. Cheng[2]

## ABSTRACT

Under the auspices of the Jet Propulsion Laboratory and the National Aeronautics and Space Administration, Hughes Aircraft Company is performing the design and development of the unmanned, lunar soft-landing spacecraft system for the Surveyor project. This paper describes the basic concept and implementation of the terminal guidance system for the landing phase.

The terminal descent profile consists of a solid rocket deboost phase with earth-based commands for thrust orientation as well as partial control of ignition. This is followed by a closed-loop vernier guidance phase with throttleable liquid engines. The automatic vernier guidance concept consists



[1]This work was performed in pursuance of Contract 950056 with the Jet Propulsion Laboratory, California Institute of Technology, under Contract No. NAS 7-100 sponsored by the National Aeronautics and Space Administration.

[2]Associate Manager, Systems Analysis Laboratory, Surveyor Program, Hughes Aircraft Company, El Segundo, California, U. S. A.

of (1) velocity magnitude control in accordance with a velocity versus slant range descent law and (2) gravity turn steering. The differential equations of motion are solved and implementation requirements obtained for anticipated variations in trajectory and site slope conditions. The on-line earth-based guidance program for solid rocket thrust attitude and ignition control is also discussed.

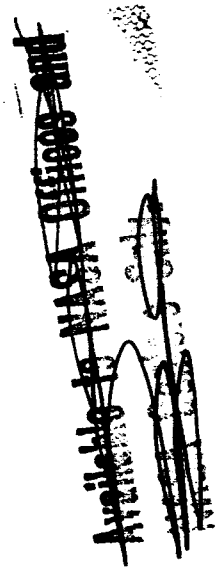

# Surveyor Terminal Guidance[1]

R. K. Cheng[2]

## I. INTRODUCTION

The Surveyor is the first U.S. project to softland an unmanned vehicle and its payload on the moon with the primary purpose of discovering those surface and environmental characteristics important to future manned lunar exploration as well as the understanding of the universe. The spacecraft, a model of which is shown in Figure 1, will be launched into a translunar trajectory with a planned midcourse correction to nullify the effects of injection errors such that the approach to the moon is a direct impact at a pre-selected landing site. The terminal slowdown begins at approximately 60 miles above the lunar surface when a pulsed radar generates a marking signal at a preset range. An earth-commanded time delay ensues and is followed by the ignition of a high thrust, solid propellant engine called the

---

[1]This work was performed in pursuance of Contract 950056 with the Jet Propulsion Laboratory, California Institute of Technoloty, under Contract No. NAS 7-100 sponsored by the National Aeronautics and Space Administration.

[2]Associate Manager, Systems Analysis Laboratory, Surveyor Program, Hughes Aircraft Company, El Segundo, California, U.S.A.

main retro. During the main retro phase, constant attitude is maintained by a set of three differentially throttling liquid vernier engines located symmetrically about the roll or thrust axis. After burnout and staging of the main retro, these same verniers are then used for removal of the remainder of the approach velocity in a closed-loop guidance mechanization involving a three-beam doppler radar for the measurement of vehicle velocity and a fourth beam for measuring slant range to the lunar surface. At a rather low altitude and a correspondingly low velocity, the vernier engines are shut off and the vehicle free falls to the surface. The landing is made with a nominally vertical attitude regardless of the slope condition.

The design of the spacecraft emphasizes simplicity and reliability. In the terminal descent and guidance system for example, the on-board radars are body-fixed, the main retro engine employs no thrust termination device, and the delicate task of soft-landing is to be achieved without the use of a digital computer. A prior paper, Reference 1, discussed some of the pertinent design considerations especially concerning approach trajectory and main retro burnout constraints arising due to propulsion and sensing limitations, and their implications with regard to fuel and guidance requirements. In this paper, the guidance mechanization, both in terms of the on-board as well as earth-based portions, is discussed and certain characteristics of interes are obtained through the solution of relatively simple though idealized equations of motion.

## II. MECHANIZATION

### Ground Computation and Command

Doppler and angle tracking data from earth-based stations will be sent to the Space Flight Operations Facility in Pasadena, California, for precise orbit determinations and guidance computations during the trans-lunar flight. Several hours prior to the vehicle's anticipated impact on the lunar surface, a final orbit determination is made which yields, besides other data, the best estimate of the unbraked impact velocity magnitude, direction, and incidence angle with respect to the lunar surface. This information is fed into a terminal guidance program, the block diagram of which is shown in Figure 2. An iterative procedure based on satisfying a simple relationship between the main-retro burnout velocity and altitude yields the nominal ignition altitude as well as the pointing direction of the thrust vector. Given that the pulse radar is preset to generate a marking signal at a given slant range, it is a relatively simple matter then to compute the time delay which must be implemented between the mark and the proper instant for engine ignition. The time delay is telemetered from earth, stored in the flight control programmer of the vehicle, and counted down automatically by the programmer upon reception of the marking signal from the radar.

The other guidance function, that of orienting the vehicle to the proper thrusting attitude, is accomplished by sequentially torquing a set of strapped-down integrating rate gyros through computed angles. The initial orientation of the spacecraft is in this case determined by the vehicle-to-sun and vehicle-to-Canopus directions which are sensed by on-board

celestial sensors. Since the thrusting direction in inertial coordinates is obtained from the terminal guidance program, the conversion into spacecraft rotation angles is a straight forward computation. The commands will be sent to and executed by the spacecraft many minutes before the anticipated ignition instant to allow for a period in which television pictures of the surface being approached may be transmitted back to earth for future analysis.

Main Retro Phase

The principal features of the main-retro phase are:

1. Constant attitude
2. Open-loop burning - no thrust control
3. Burning to fuel depletion - no thrust termination

The only on-board guidance instrumentation, aside from the strapped-down gyros needed for sensing attitude changes and causing the vernier engines to throttle differentially to counteract such changes, is a crude longitudinal acceleration switch which senses the decay of thrust and initiates a fixed-duration separation sequence.

The conditions at the end of the separation period, also called the burnout conditions, determine to a large degree the satisfactory operation of the subsequent vernier descent phase, assuming that no malfunction occurs. The chief constraints on the altitude as well as the magnitude and direction of the velocity vector arise due to propulsion and terminal sensor limitations as discussed in Reference 1.

The altitude constraint is a function of velocity, the lower limit being further determined by the maximum thrust/weight capability and the

upper limit by the amount of propellant remaining. The velocity magnitude is limited approximately to the interval of 150 to 650 ft/sec. The flight path is restricted to a cone of 45° half-cone angle about the local vertical in order to ensure proper incidence of the doppler radar beams on the lunar surface once the gravity turn steering begins. The actual burnout velocity for a given flight even with the effects of the variability in the translunar trajectory and midcourse correction and dispersions in the main-retro phase taken into account, still has a very high probability of being within the indicated allowable range. The actual burnout altitude is determined by the earth-commanded setting of the ignition delay and main-retro phase dispersions. If there were no dispersions, the burnout altitude would be at a value specified by a function, called the "Nominal Burnout Locus", of the magnitude of the predicted nominal burnout velocity. The locus is designed as a compromise between fuel consumption and clearance above a minimum altitude which can be handled by the limited acceleration capability of the vernier engines, allowing for the random dispersions about any given operating point on the locus. A graph of the burnout locus, dispersion ellipses and constraint contours which illustrate the design problem is shown in Figure 3.

Vernier Phase

The heart of the vernier guidance mechanization is the RADVS (Radar Altimeter Doppler Velocity Sensor) system, the beam geometry of which is shown in Figure 4. There are two split beam antennas placed near the bottom of the vehicle basic framework. Antenna 1 supplies one of the three doppler beams as well as the altitude beam (more appropriately, the slant range along the thrust direction). Antenna 2 supplies the other two doppler beams. The doppler beams are directed at three corners of a square and all are located at an equal angle $\theta$ away from the thrust axis. The shift in frequency of the return from that of the transmitted signal is proportional to the spacecraft velocity multiplied by the cosine of the angle between the velocity vector and the beam direction. Referring to Figure 4.

$$V_1 = \frac{c\Delta f_1}{f_o} = \frac{V_x \sin\theta}{\sqrt{2}} + \frac{V_y \sin\theta}{\sqrt{2}} + V_z \cos\theta \qquad (1)$$

$$V_2 = \frac{c\Delta f_2}{f_o} = -\frac{V_x \sin\theta}{\sqrt{2}} + \frac{V_y \sin\theta}{\sqrt{2}} + V_z \cos\theta \qquad (2)$$

$$V_3 = \frac{c\Delta f_3}{f_o} = -\frac{V_x \sin\theta}{\sqrt{2}} - \frac{V_y \sin\theta}{\sqrt{2}} + V_z \cos\theta \qquad (3)$$

From Equations (1), (2) and (3), the velocity components along the vehicle fixed coordinate system may be solved

$$V_x = \frac{V_1 - V_2}{\sqrt{2}\sin\theta} \qquad (4)$$

$$V_y = \frac{V_2 - V_3}{\sqrt{2} \sin \theta} \tag{5}$$

$$V_z = \frac{V_1 + V_3}{2 \cos \theta} \tag{6}$$

It may be seen that this particular beam geometry results in the algebraic summing or differencing of only two quantities for each of the three components of velocity along x, y, z. Thus, it permits direct frequency mixing of the return signals in pairs, a distinct simplification in mechanization than in the case where the beams are symmetrically located (at 120° azimuth separation) around the thrust axis.

The altimeter transmits a CW signal modulated in frequency by a triangular wave. The return wave shape is shifted in time by an amount equal to

$$\Delta t = \frac{2R}{c} \tag{7}$$

If the two frequencies are differenced, the result is a wave represented by the dotted function in Figure 5. The portion above the reference abscissa axis has a height, in the case of zero relative velocity between the radar and the target, proportional to the range along the beam. In the actual situation, the doppler shift adds an additional frequency shift proportional to $V_z$. This, however, is easily removed in the data processing circuitry since $V_z$ is itself obtainable by mixing two of the three doppler beam frequencies.

The outputs of the RADVS are $V_x$, $V_y$, $V_z$ and R, in the form of analog voltages. The first two of these are used to generate pitch and yaw steering commands and the last two for thrust acceleration control.

The flight control system block diagram showing all of the important elements active during the vernier descent phase is shown in Figure 6. The $V_x$ and $V_y$ signals are used to torque the strapped-down yaw and pitch rate-integrating gyros. The slant range signal R is fed into a function generator which generates a corresponding required velocity $V_R$. The difference between $V_R$ and $V_Z$ is defined as the velocity error. It is amplified and limited before becoming the thrust acceleration command signal. The output of a longitudinal accelerometer is compared with this signal and the difference is eventually used to raise or lower the thrusts of all three engines by the same amount. Returning to the pitch and yaw channels, the rate errors are integrated by the gyros, then amplified and fed into a mixing network which also accepts the thrust acceleration error signal. The three inputs to the network determine the three outputs which are the thrust commands to the engines. Finally, the vehicle dynamical geometrical relations complete the feedback to the RADVS and the accelerometer.

## III. VERNIER GUIDANCE CHARACTERISTICS

### Basic Guidance Concept

The basic concept used in the vernier guidance system involves; (1) gravity turn steering throughout the descent immediately following RADVS acquisition of the velocity vector and (2) a minimum acceleration phase followed by guiding along a nominal descent contour of V vs R for the generation of velocity error which in turn is used to control the thrust acceleration.

The use of gravity turn steering has several outstanding advantages. First, because of the fact that the thrust axis is required to be colinear with the velocity vector which, as was shown earlier, is easily obtained in body coordinates, there is no requirement for the knowledge of another direction. In any other steering scheme, the knowledge of the direction of local vertical is generally necessary, either explicitly or unexplicitly, resulting in more complex instrumentation. Secondly, the gravity turn descent has a very desirable property that,as the velocity approaches zero, the flight path (thus also thrust direction) tends towards the vertical. No violent reorientation maneuver is needed prior to touchdown. Thirdly, a gravity turn with suitable thrust acceleration control is an efficient trajectory fuel wise for a wide range of initial flight path angles ranging from near horizontal to vertical.

In the thrust acceleration control channel, the use of a nominal V vs R descent trajectory permits near maximum utilization of the vernier thrust capability. The transition from burnout to this mode of descent is via a minimum acceleration descent rather than a complete shutoff of the vernier engines because of the necessity of maintaining attitude stabilization for proper sensor operation.

Doppler and range acquisition by the RADVS is anticipated during the minimum acceleration phase. As long as the measured state of the vehicle, represented as a point in the velocity-range phase plane, is well above the descent contour, the acceleration is constant at a level determined by the minimum thrust capability of the engines as well as the anticipated weight of the spacecraft.

The major portion of the descent contour is an approximation of the idealized parabolic relation:

$$R = \frac{V^2}{2(n-1)g} \tag{8}$$

which, in the case of vertical descent, requires a constant thrust acceleration equal to ng. Later it will be shown that for a fairly wide range of flight path as well as average surface slope condition, the acceleration requirement does not differ appreciably from ng. This is consistent with the general desire to find a simple guidance law which could cope with a wide range of anticipated conditions while, at the same time, yield nearly maximum performance within the available thrust constraint.

The contour near the origin of the R-V plane deviates from that given by Equation 8. A constant low velocity descent phase is incorporated which serves to absorb altitude errors when the spacecraft velocity reaches this value. Finally, engine shutoff is made when the range beam indicates a specific value (different from zero), in order to avoid possible detrimental effects resulting from the impingement of rocket exhaust on the surface.

Differential Equations

Referring to Figure 7, the basic differential equations for a gravity turn descent with an arbitrary thrust acceleration (not necessarily constant) are

$$\frac{dV}{dt} = \dot{V} = - a + g \cos \psi \tag{9}$$

$$V \frac{d\psi}{dt} = V\dot{\psi} = - g \sin \psi \tag{10}$$

These equations may or may not yield closed form solutions depending on the nature of the accelerations or indirectly, the particular longitudinal guidance law chosen.

Minimum Acceleration Phase

During the minimum acceleration phase which links the operation along the descent contour with main-retro burnout, the behavior is very simply solved by noting that in Equation (9)

$$a = n_{min}\, g \tag{11}$$

Thus, by dividing (9) by (10) we obtain

$$V \frac{dV}{d\psi} = \frac{n_{min} - \cos \psi}{\sin \psi} \tag{12}$$

In the interest of conserving fuel, $n_{min}$ is chosen to be somewhat less than unity. For $\psi$ lying somewhere between zero and 90° it is therefore possible for $\frac{dV}{d\psi}$ to be either positive or negative. If initially $\cos \psi$ is less than $n_{min}$ V tends to decrease with time at first. This trend in most cases however is

reversed because the decreasing value of $\psi$ will soon cause $\frac{dV}{dt}$ to change sign.

Integration of Equation (12) results in

$$\frac{V}{V_o} = \left( \frac{\tan \frac{\psi}{2}}{\tan \frac{\psi_o}{2}} \right)^{n_{min}-1} \frac{\sec^2 \frac{\psi}{2}}{\sec^2 \frac{\psi_o}{2}} \tag{13}$$

where the subscript "0" denotes initial values. The factor

$$g(\psi) = \left( \tan \frac{\psi}{2} \right)^{n_{min}-1} \sec^2 \frac{\psi}{2} \tag{14}$$

which may be called the "velocity integral" is plotted in Figure 8 for various values of $n_{min}$. The Surveyor design presently has $n_{min} = 0.9$. As a result $g_{min}$ occurs at $\psi = \cos^{-1} n_{min} = 25.8°$, the point at which $\frac{dV}{dt}$ passes through zero. The phase plane behavior is illustrated in Figure 9 for values of $\psi_o$ on either side of $\cos^{-1} n_{min}$.

Intersection with Descent Contour

The minimum acceleration phase is terminated when the measured slant range reaches a value given by Equation (8). The altitude $h_a$ at this point is a function not only of velocity but also of flight path angle

$$h_a = \frac{V_a^2}{2(n-1)g} \cos \psi_a \tag{15}$$

The exact point of intersection is solvable by the iterative formula

$$\tan\frac{\psi_a}{2} = \tan\frac{\psi_o}{2}\left[\frac{\frac{n - n_{min}}{(1 - n_{min})(n - 1)} - \left(\tan\frac{\psi_a}{2}\right)^4 \frac{n_{min} - n + 2}{(n - 1)(n_{min} + 1)}}{\frac{2gh_o}{V_o^2}\left(\sec\frac{\psi_o}{2}\right)^4 + \frac{1}{1 - n_{min}} + \frac{\left(\tan\frac{\psi_o}{2}\right)^4}{1 + n_{min}}}\right]^{\frac{1}{2(1 - n_{min})}} \tag{16}$$

which may be used with (13) and (15) for the complete determination of the intersection point. In general, $\psi_a$ is always less than $\psi_o$ due to the effect of the gravity turn steering while $V_a$ may be either higher or lower than $V_o$. In the case of Surveyor, there is a high probability that $V_a$ will not differ from $V_o$ by more than 50 feet per second or so, due to the fact that $n_{min}$ is so close to being unity.

Idealized Behavior Along Descent Contour

The idealized behavior along the Descent Contour may be found by the following procedure. Noting first from the geometry shown in Figure 7 that

$$R = h \sec\psi \tag{17}$$

we differentiate Equation (17) with respect to time,

$$\dot{R} = \dot{h} \sec\psi + h\dot{\psi} \sec\psi \tan\psi \tag{18}$$

But,

$$\dot{h} = - V \cos \psi \tag{19}$$

Also,

$$h = \frac{V^2}{2 (n - 1) g} \cos \psi \tag{20}$$

Thus

$$\dot{R} = - V + \frac{V^2 \dot{\psi}}{2 (n - 1) g} \tan \psi \tag{21}$$

which, in view of Equation (10), becomes

$$\dot{R} = - V \left[ 1 + \frac{1}{2 (n - 1)} \sin \psi \tan \psi \right] \tag{22}$$

Now, if Equation (8) is differentiated with respect to time

$$\ddot{R} = \frac{V \dot{V}}{2 (n - 1) g} \tag{23}$$

Equations (22) and (23) are combined to eliminate $\dot{R}$

$$\dot{V} = - \left[ (n - 1) g + \frac{1}{2} \sin \psi \tan \psi \right] \tag{24}$$

If Equation (24) is divided by Equation (10), the dummy variable time is eliminated and we have the key differential equation relating velocity and flight path angle

$$\frac{d V}{d \psi} = \frac{n - 1}{\sin \psi} + \frac{1}{2} \tan \psi \tag{25}$$

which may be integrated to yield the general solution

$$\frac{V}{V_a} = \left( \frac{\tan \frac{\psi}{2}}{\tan \frac{\psi_a}{2}} \right)^{n - 1} \left( \frac{\sec \psi}{\sec \psi_a} \right)^{\frac{1}{2}} \tag{26}$$

a result differing from the constant-acceleration gravity-turn solution only in the exponent of the secant term.

The numerator of the right-hand side of Equation (26) is plotted in Figure 10 for several representative values of n including the case of n = 2, very nearly the Surveyor characteristic. No startling behavior is exhibited here. It is seen that velocity decreases monotonically as $\psi$ becomes smaller.

Of greater interest is the thrust acceleration required to follow the Descent Contour. From Equation (9)

$$a = g \cos \psi - \dot{V} \tag{27}$$

But $\dot{V}$ is given by Equation (24), thus

$$a = ng + (\cos \psi + \frac{1}{2} \sin \psi \tan \psi - 1)\, g = ng + \frac{(1 - \cos \psi)^2}{2 \cos \psi}\, g \tag{28}$$

Equation (28) shows that the required thrust acceleration depends on $\psi$ only. The second term in the right-hand side, plotted in Figure 11, is the excess acceleration required above the nominal value of n. The interesting and important property of this term is its negligibly small magnitude compared to g, for $\psi$ ranging from zero up to even as high as 45°. Thus, for all practical purposes, the thrust acceleration required may be regarded as a constant. In the design of the Surveyor, the Descent Contour is therefore made to correspond to a value of thrust acceleration just slightly less than the maximum capability.

In the case where a surface slope $\mu$ exists in the direction of travel, the acceleration required may be shown to be

$$a = ng + \left[\cos \psi + \frac{1}{2} \sin \psi \tan (\psi - \mu) - 1\right] g \qquad (29)$$

where a positive $\mu$ indicates an uphill approach. Thus, the acceleration required tends to be greater for the downhill case where $\mu$ is negative. It is not difficult to see from physical interpretation that this must be true. As the gravity turn bends the trajectory towards the vertical, the slant range tends to decrease more rapidly in the downhill than in the uphill situation. Correspondingly in the former case a higher thrust acceleration is demanded of the system.

The choice of n, the nominal descent contour acceleration level, given that there is a maximum capability $n_{max}$, is determined by a "slope-flight path" capability equation

$$\tan \mu = \left[\frac{4 n_{max}^2 - 1}{4(n_{max}^2 - 1)}\right] \left[\frac{2(n-1)(1 + 2 n_{max} \cos \psi + \cos^2 \psi) - 4(n_{max}^2 - 1) \cos \psi}{4 n_{max}^2 - 1 - 2(n-1)(2 n_{max} + \cos \psi)}\right] \csc \psi \qquad (30)$$

Figure 12 is a plot of $\mu$ versus $\psi$ for $n_{max} = 2.35$ and various values of n. It turns out that the capability curve is a strong function of $n_{max} - n$, the acceleration margin between the maximum capability and the nominal descent acceleration (in the vertical case). In the actual design, allowance must also be made for sensor and electronic errors which may be lumped together as an equivalent dispersion in n. A margin of 0.25 to 0.30 lunar g is found to be required for the Surveyor system.

Another interesting property of the trajectory is the manner the turning rate $\dot{\psi}$ varies as V approaches zero. From Equations (10) and (26),

$$\dot{\psi} = -\frac{g}{V} \sin \psi$$

$$= -g \sin \psi \left( \frac{\tan \frac{\psi}{2}}{\tan \frac{\psi_a}{2}} \right)^{1-n} \left( \frac{\sec \psi}{\sec \psi_a} \right)^{-\frac{1}{2}} \qquad (31)$$

since V and $\psi$ approaches zero together,

$$\lim_{V \to o} \dot{\psi} = \lim_{\psi \to o} \dot{\psi}$$

$$= \lim_{\psi \to o} c \psi^{2-n} \qquad (32)$$

where c is a constant. Thus, there are three possibilities:

1. If $n < 2$, $\dot{\psi}$ approaches zero
2. If $n = 2$, $\dot{\psi}$ approaches a non-zero constant
3. If $n > 2$, $\dot{\psi}$ diverges

The last possibility presents a problem at least in the idealized sense if we attempt to follow the gravity turn to zero velocity. In practice, however, two things can be done to alleviate the situation (a) use of a lower acceleration level near V = 0 or, (b) incorporate inertial hold at some finite velocity and accept a small residual horizontal velocity component. Both are implemented in the Surveyor design although not primarily for the above reason.

Straight-Line Approximation of Descent Contour

Equation (8) is not exactly implemented in the spacecraft. Rather, a 4-segment straight line approximation of this equation, shown in Figure 13 and actually furnished by a diode function generator, is used instead.

Because of the finite number of segments, there are some deviations in behavior from those characterizing the idealized case, the chief difference being the presence of thrust acceleration saturation periods when the system attempts to follow the Descent Contour. This behavior, discussed in Reference 1, has the beneficial effect of shielding the longitudinal guidance channel from radar noise at least during most of the acceleration-saturated portions. However, towards the bottom end of each segment, close tracking should and does occur.

Taken as a whole, the straight-line mechanization yields practically the same results with regard to fuel consumption and flight path angle reduction as the idealized case.

The actual thrust acceleration command is derived as shown in Figure 14, with the resultant characteristic of Figure 15. The width of the linear region of operation $\frac{(\Delta \hat{a})_{max}}{K_v}$ is of the order of a few feet per second.

Final Segment and Touchdown

The operation along the final segment to actual touchdown consists of several important features which deserve some discussion.

The final segment design has it passing through the origin in the R - V plane as shown in Figure 16. However, the portion near the origin is not used for guidance, as it is easy to show that following a straight line to the origin is not physically realizable from the fuel requirement standpoint. Instead, a constant-velocity (of nominally $V_c$ = 5 ft/sec) descent subphase is implemented prior to engine shutoff. This also means that altitude dispersions which exist at the beginning of this subphase will produce a

negligible effect on the landing velocity. Another discrete change in implementation from the pure gravity-turn mode is the use of inertial attitude hold at a slightly higher velocity $V_b$ of say 10 ft/sec, thus effectively removing the radar inputs to the lateral channel at these very low velocities where radar noise might produce jerky attitude changes. Simultaneously the velocity command is switched to the constant value of $V_c$.

When the vehicle state reaches $P_o$ the top of the final segment, the flight path angle in general has been reduced to a small enough value (< 20°) so that small angle approximations may be used to solve for the behavior from this point onward. The thrust acceleration is saturated at first with a value equal to $n_{max}$ g and the velocity-flight path relationship is approximately

$$\frac{V}{V_o} = \left(\frac{\dot{\psi}}{\dot{\psi}_o}\right)^{n_{max} - 1} \tag{33}$$

Also,

$$V_o^2 - V^2 \cong 2g(n_{max} - 1)(R_o - R) \tag{34}$$

At the point where the thrust acceleration comes out of saturation, the trajectory "acquires" the straight line and begins to track it. If b is defined as the slope of the segment, or

$$b = \frac{R}{V} \tag{35}$$

it may be noted from Equation (34) that the acquisition velocity $V_a$ must satisfy the equation

$$V_o^2 - V_a^2 = 2g\,(n_{max}-1)\,(bV_o - bV_a) \tag{36}$$

Solving for $V_a$

$$V_a = 2bg\,(n_{max}-1) - V_o \tag{37}$$

$V_a$ must in practice be a value somewhat higher than $V_b$, the point at which the commanded velocity is switched to $V_c$. This implies that b must be larger than some positive constant

$$b > \frac{V_b + V_o}{2g\,(n_{max}-1)} \tag{38}$$

On the other hand, it may be shown that the fuel requirement from $V_a$ to $V_b$ is

$$\Delta V = V_a - V_b + bg \ln \frac{V_a}{V_b} \tag{39}$$

The gravity loss term is thus directly proportional to b, which must not therefore be excessively large.

The value of b also influences the spacecraft flight path angle at $V_b$. Since ideally the attitude coincides with the flight path, this angle must be kept small so that the subsequent thrust velocity increment does not give rise to an excessive horizontal velocity component.

During the "tracking" phase from $V_a$ to $V_b$, the behavior is described by the following differential equation

$$\frac{dV}{d\psi} = \frac{V^2}{bg} \csc \psi + V \tan \psi \tag{40}$$

the solution of which is

$$V \cos \psi = \frac{V_a \cos \psi_a}{1 + \frac{V_a \cos \psi_a}{bg} \ln \left( \frac{\tan \psi_a}{\tan \psi} \right)} \tag{41}$$

For small angles, Equation (41) may be shown to be equivalent to

$$\frac{\psi}{\psi_a} \simeq e^{-\left( \frac{V_a - V}{V} \right) \frac{bg}{V_a}} \tag{42}$$

Thus, the value of b needs to be large in order that the above ratio, evaluated at $V_b$ be as small as practically possible.

The above considerations lead to a choice of b which is a compromise between fuel cost on the one hand and final flight path off vertical on the other.

When the state reaches B with a velocity of $V_b$, the switching of the commanded velocity to a constant value of $V_c$ momentarily causes saturation of thrust acceleration of the system, but within a very short altitude decrement the velocity of $V_c$ is essentially attained. The subsequent descent to point C removes any initial altitude dispersion except for that component which is common to the engine cutoff mechanization.

Engine cutoff is commanded when the RADVS indicates a preset range of $R_c$. The choice of $R_c$ (equal to 13 feet in the actual mechanization) is a compromise between rocket exhaust interaction and touchdown velocity considerations.

The vehicle lands with a vertical velocity determined primarily by the cutoff altitude and secondarily by the actual velocity during the constant-velocity descent. Both these parameters, aside from their obvious dependence on the nominal settings, are chiefly determined by the RADVS measurement. Likewise, in the lateral channel the horizontal velocity component is primarily caused by three sources:

1. Residual attitude, differing from vertical due to radar noise effect, at $V_b$.
2. Residual attitude due to terminating gravity turn steering at finite velocity.
3. Thrust to RADVS misalignment.

The noise effect turns out to be the most important as shown by analyses.

# IV. CONCLUDING REMARKS

The principal characteristics of the Surveyor Terminal Guidance System, discussed in the preceding sections, have shown that a simple concept with a resulting simple mechanization can be used to solve what might appear at first to be a complex problem. The fact that a number of the characteristics of interest can be deduced in simple, analytical forms is of enormous help in actually specifying numerical performance requirements for the subsystems. It is a firm belief of the author, biased it may be, that a concept resulting in mathematically simple behavior has a definite advantage over those which can only be analyzed numerically on a computer. It is fortunate that such a concept is available for the design of the Surveyor.

Nomenclature

| | |
|---|---|
| $V_1$, $V_2$, $V_3$ | velocity along doppler beams 1, 2 and 3 respectively |
| $\Delta f_1$, $\Delta f_2$, $\Delta f_3$ | frequency shifts corresponding to above |
| c | velocity of light |
| $f_o$ | transmitted frequency |
| X, Y, Z, | body-fixed cartesian coordinates |
| $V_x$, $V_y$, $V_z$ | velocity along the X, Y, and Z axes |
| $\theta$ | beam to thrust axis angle |
| R | slant range |
| V | magnitude of velocity |
| g | lunar surface gravitational attraction |
| n | nominal thrust to lunar weight ratio |
| a | thrust acceleration |
| $\psi$ | flight path angle, with respect to vertical |
| $n_{min}$ | thrust to lunar weight ratio during minimum thrust phase |
| $\mu$ | surface slope |
| $n_{max}$ | maximum thrust to lunar weight ratio |
| $V_c$ | nominal cut off velocity |
| $R_c$ | nominal cut off altitude |
| b | slope of final segment |

FIGURE 1

MODEL OF SURVEYOR IN LANDED CONFIGURATION

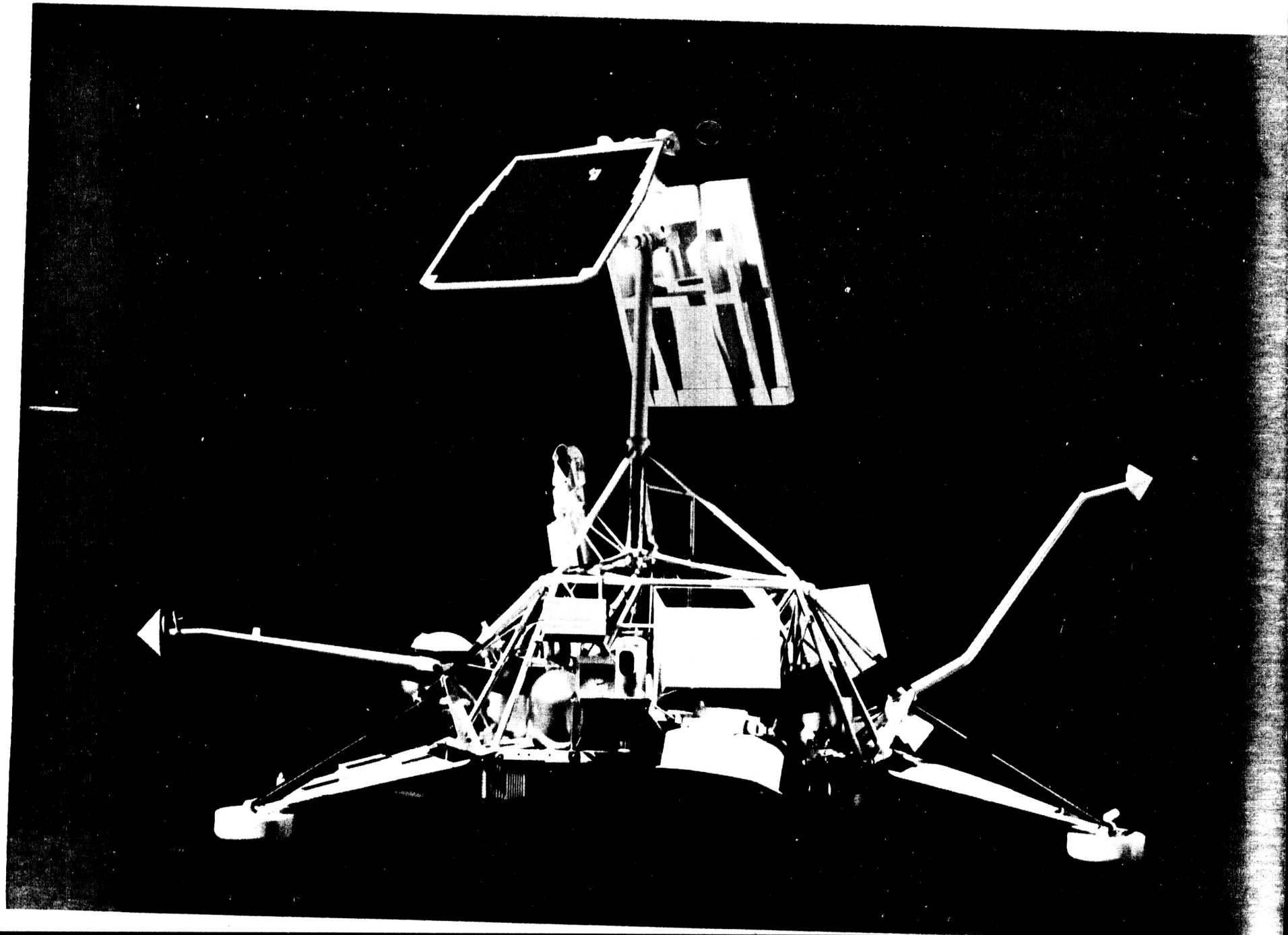

References:

1. R.K. Cheng and D.A. Conrad: Design Considerations for the Surveyor Terminal Descent System. AIAA Paper No. 64-644, presented at the AIAA/ION Astrodynamics Guidance and Control Conference, Los Angeles, California, August, 1964.

2. R. K. Cheng and I. Pfeffer: Terminal Guidance System for Soft Lunar Landing, Guidance and Control, R.E. Roberson and J.S. Farrior, editors, Academic Press, New York, 1962.

3. B.A. Kriegsman and M.H. Reiss: Terminal Guidance and Control Techniques for Soft Lunar Landing. ARS Journal, March 1962.

4. W.G. Green: Logarithmic Navigation for Precise Guidance of Space Vehicles. IRE Transactions on Aerospace and Navigational Electronics, June 1961.

5. S.J. Citron, S.E. Dunin, and H.F. Meissinger: Terminal Guidance Technique for Lunar Landing. AIAA Journal, March 1964.

6. R.K. Cheng: Lunar Terminal Guidance, Chapter 7 of Lunar Missions and Explorations, edited by C.T. Leondes and R.W. Vance, John Wiley and Sons, New York, 1964.

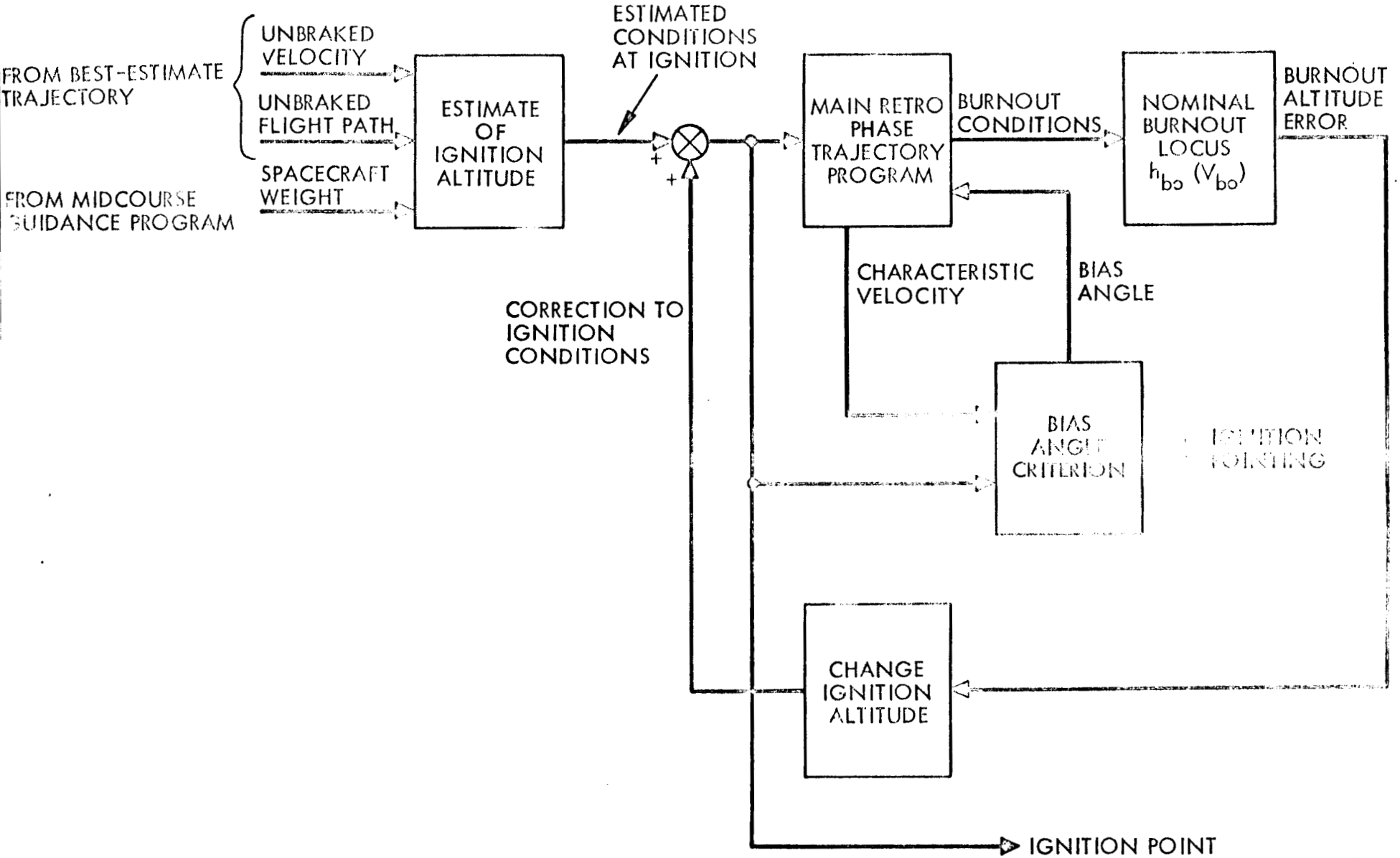


FIGURE 2. TERMINAL GUIDANCE FOR IGNITION CALCULATION

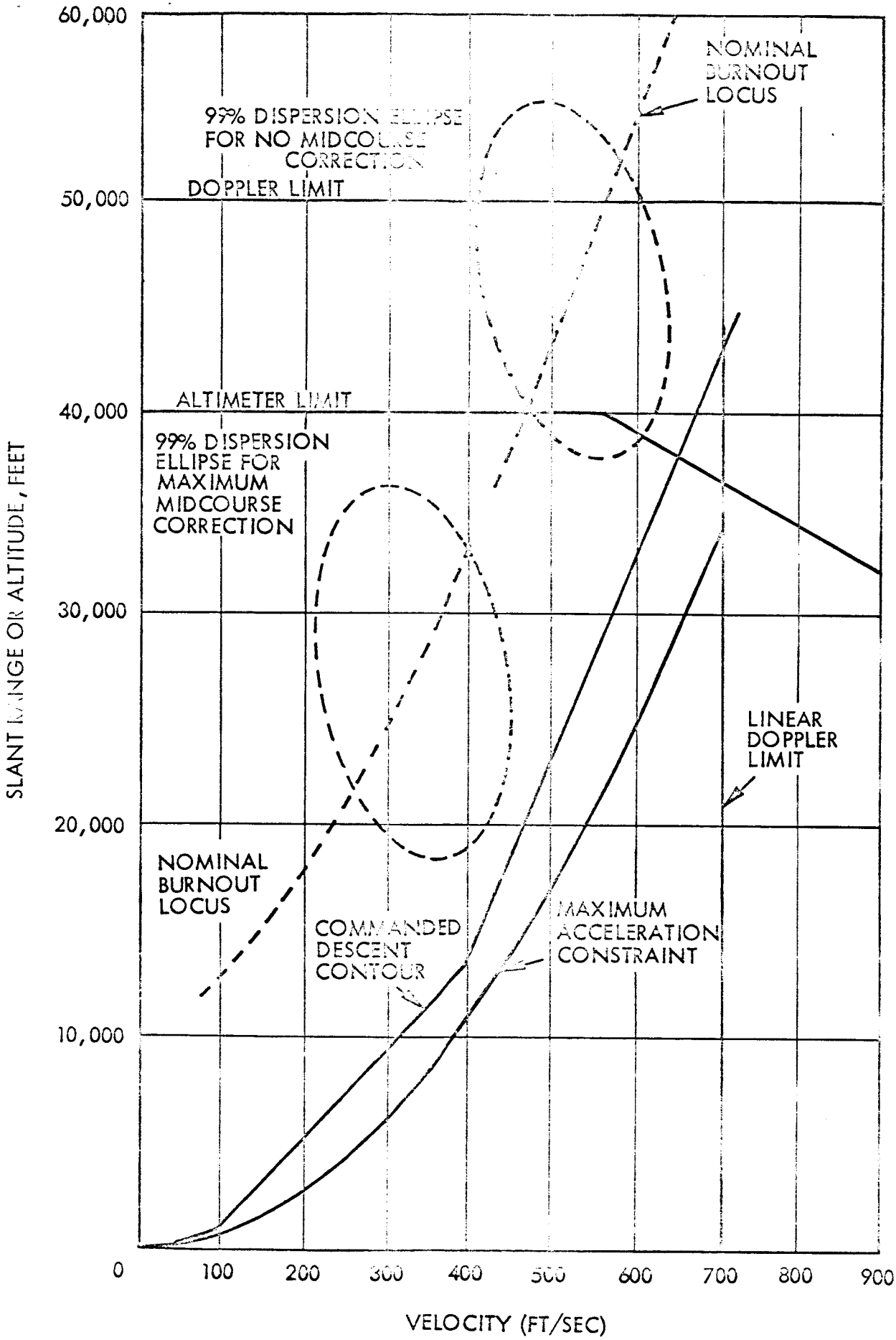


FIGURE 3. VERNIER DESCENT PHASE

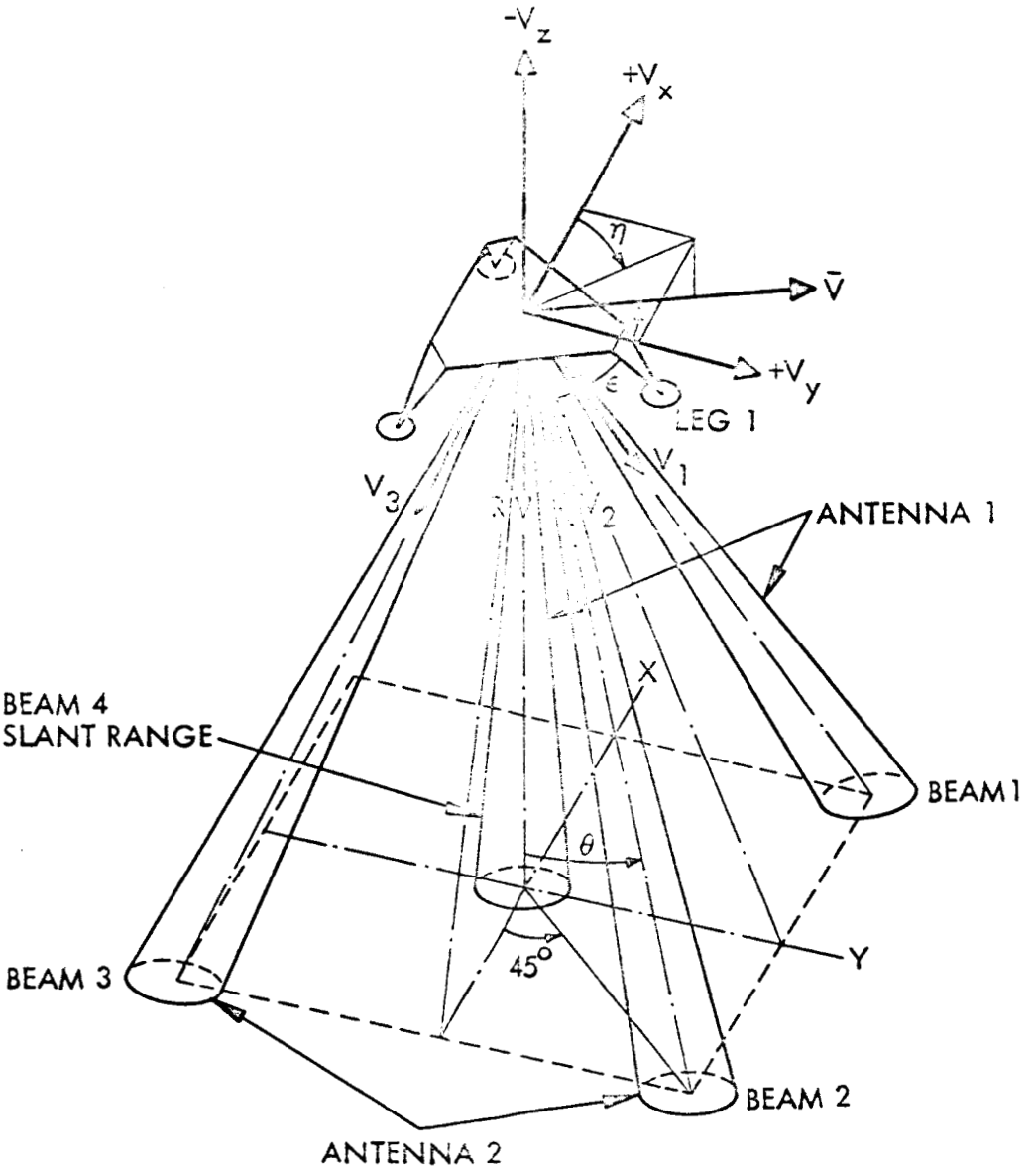


FIGURE 4. RADVS BEAM GEOMETRY

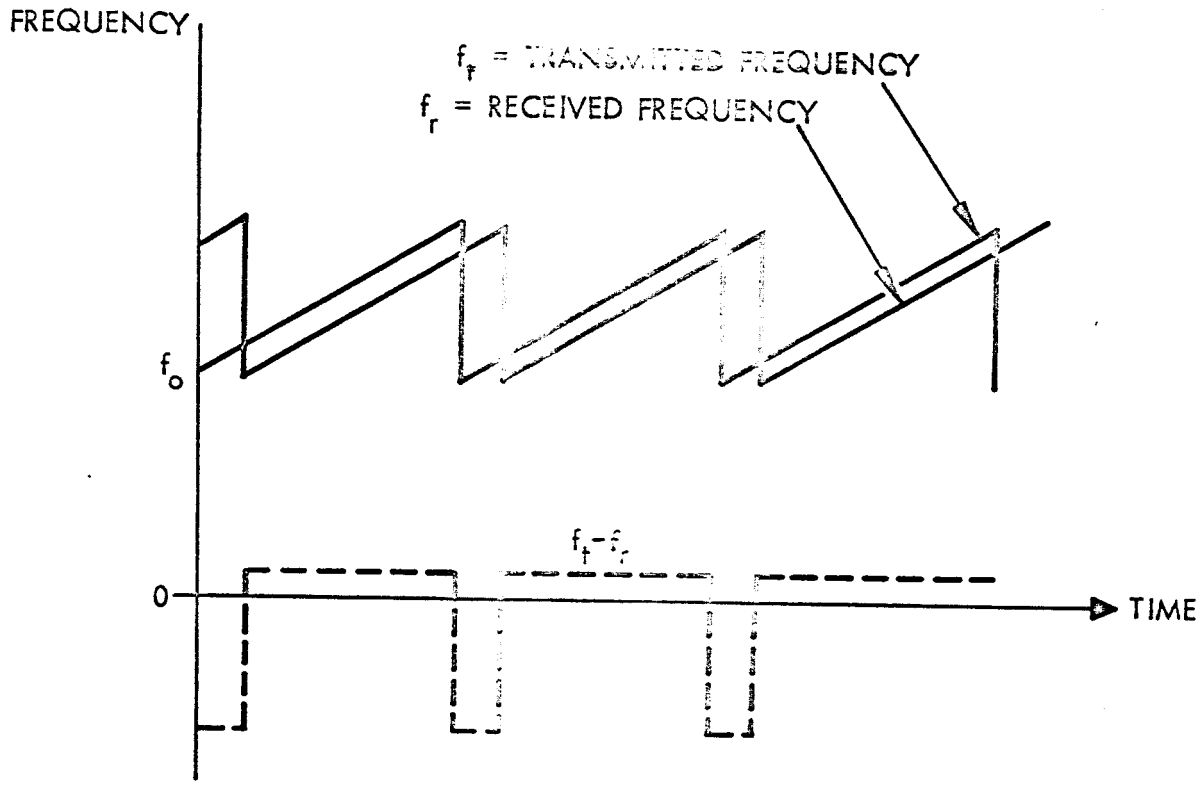


FIGURE 5. ALTIMETER SIGNALS

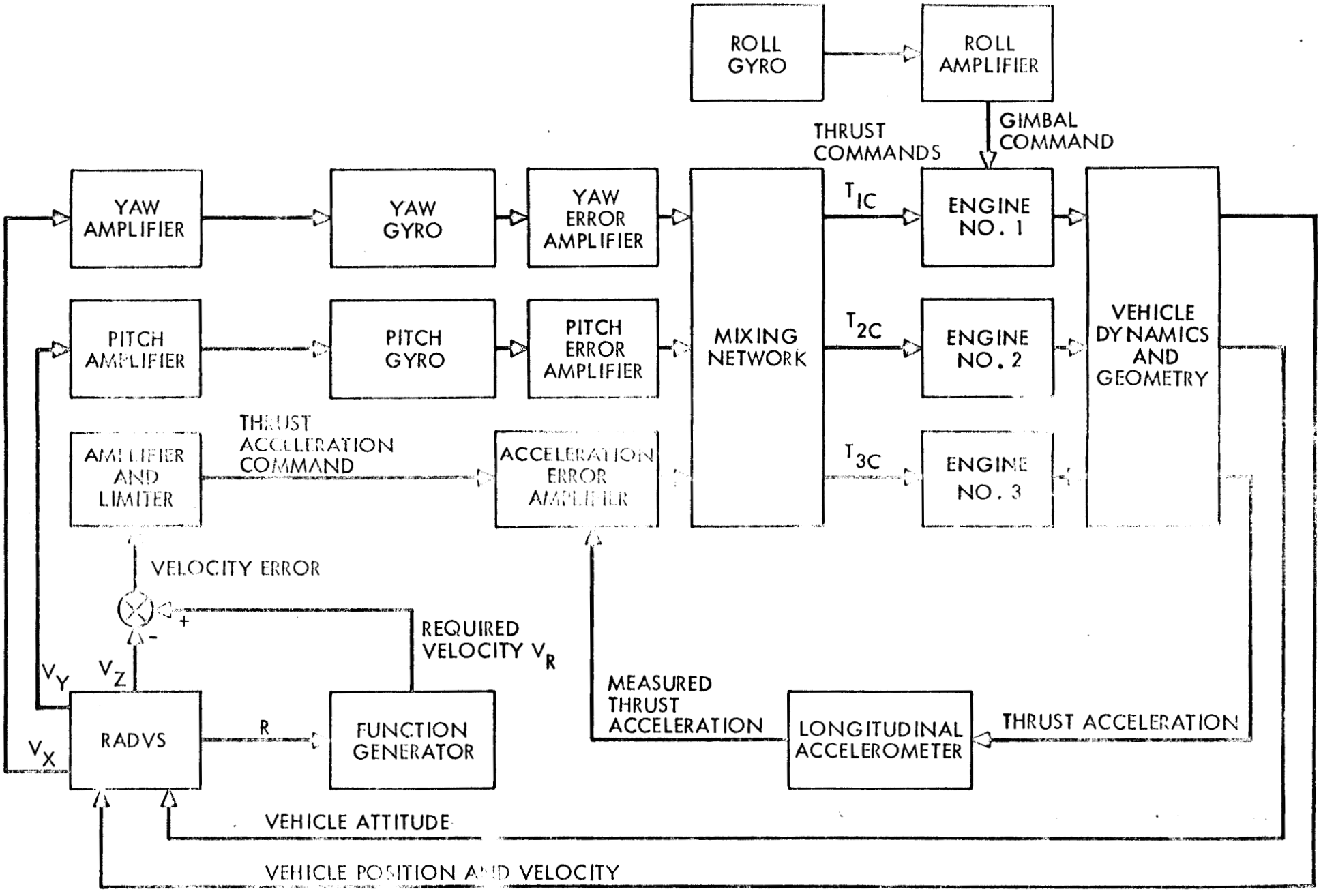


FIGURE 6. FLIGHT CONTROL SYSTEM BLOCK DIAGRAM VERNIER PHASE

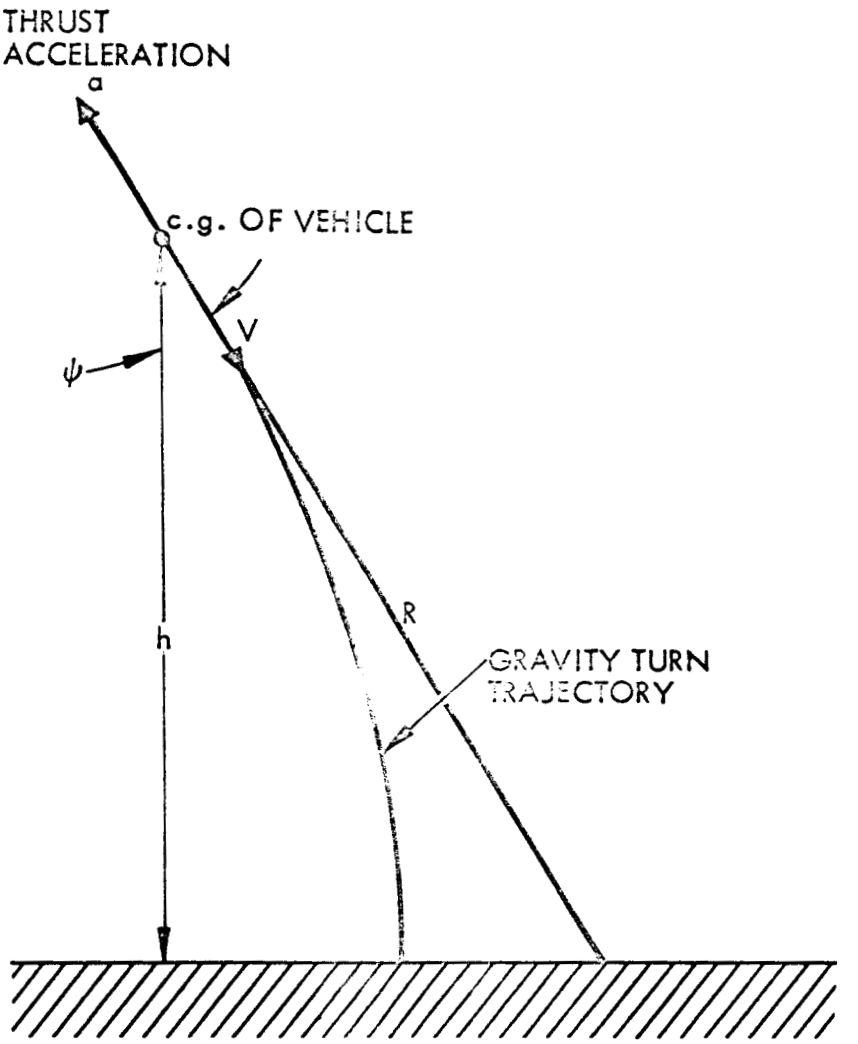


FIGURE 7. GRAVITY TURN GEOMETRY

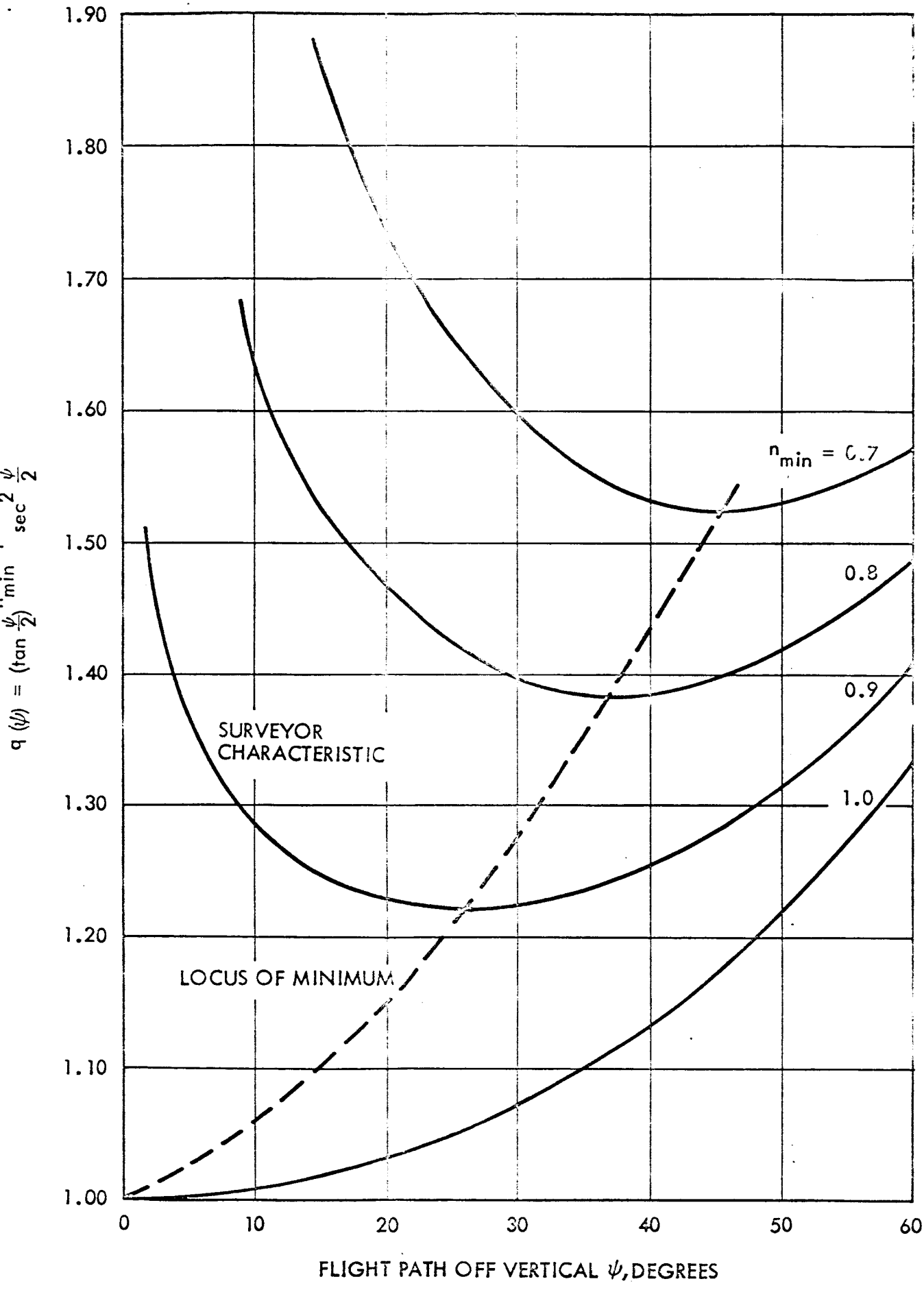


FIGURE 8. VELOCITY INTEGRAL FOR MINIMUM ACCELERATION PHASE

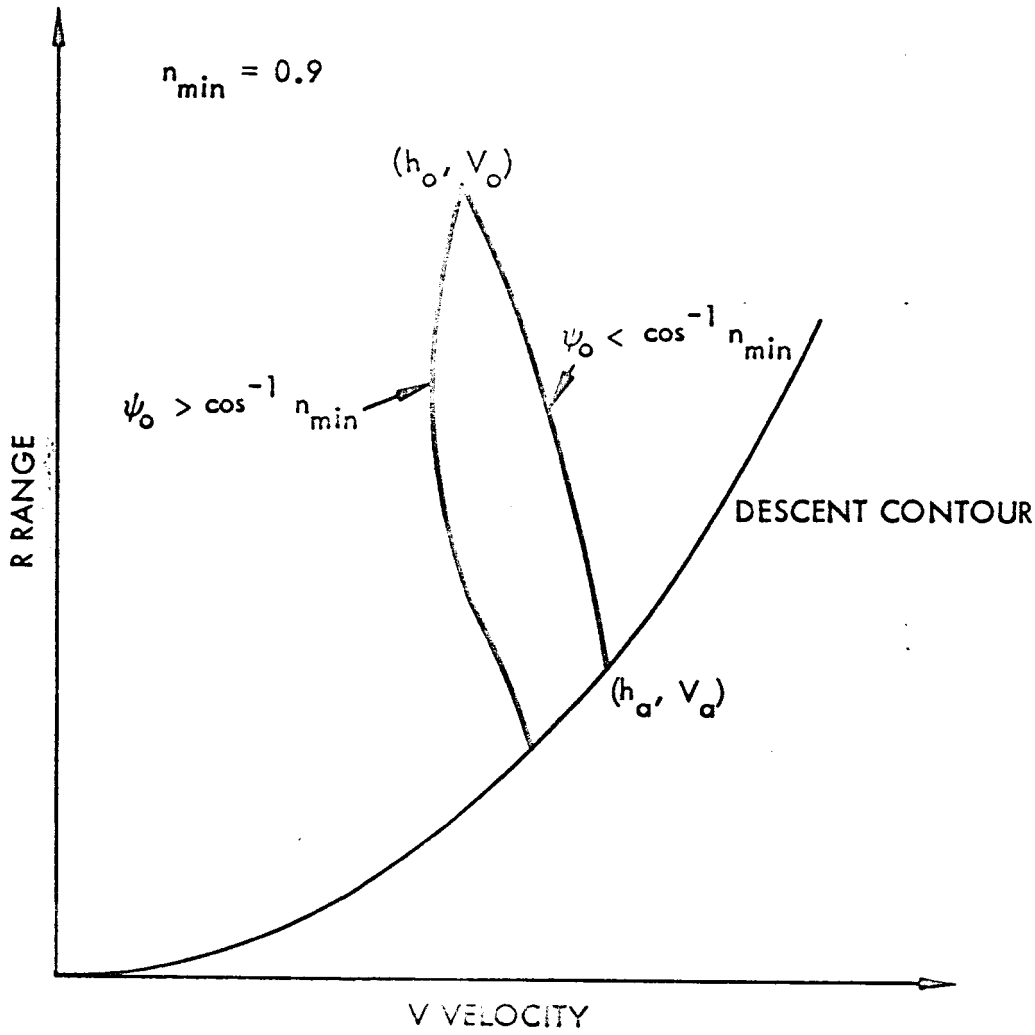


FIGURE 9. TWO POSSIBLE BEHAVIORS DURING MINIMUM ACCELERATION PHASE

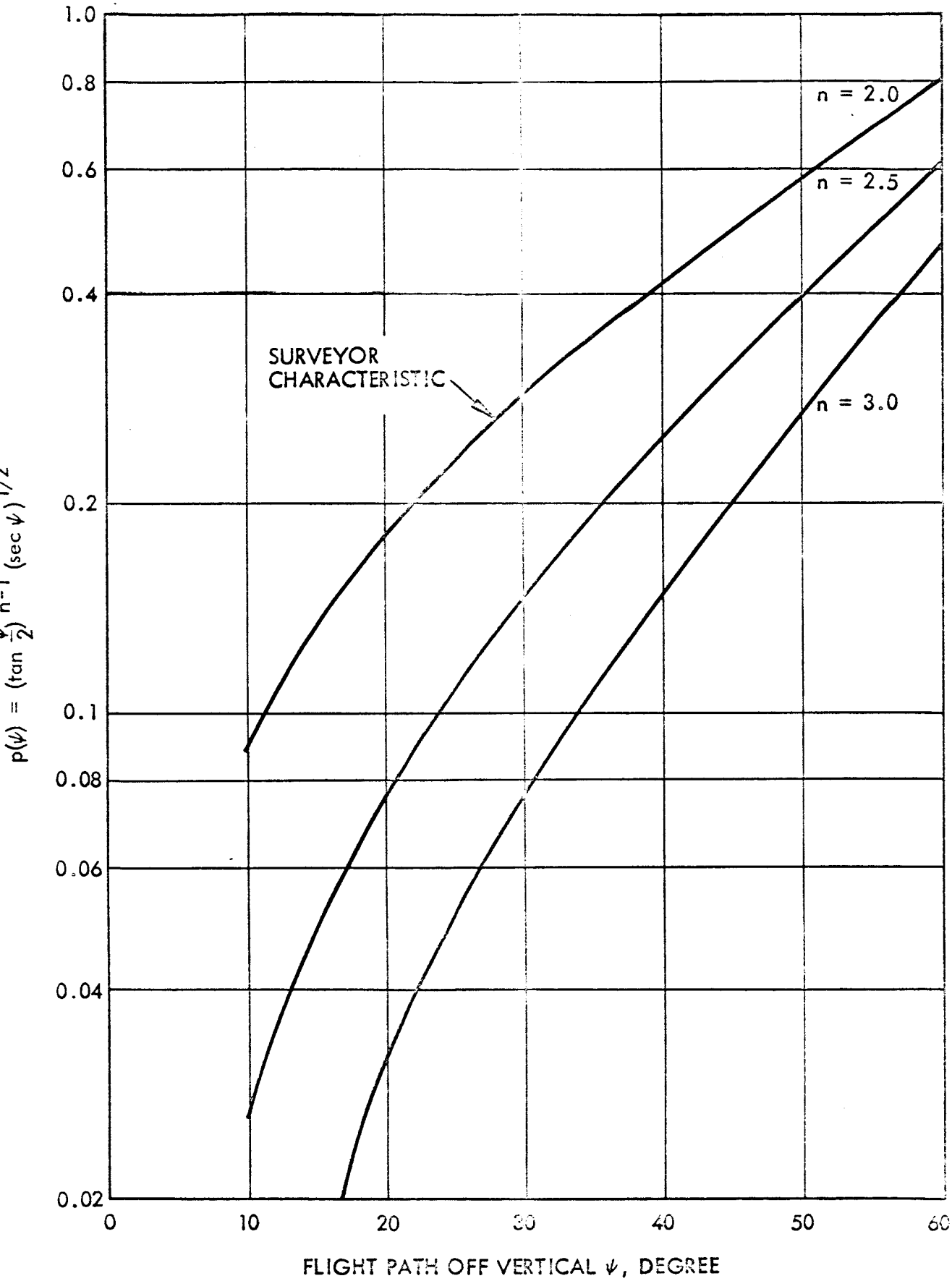


FIGURE 10. VELOCITY INTEGRAL FOR CONSTANT - $V^2/R$ GRAVITY TURN

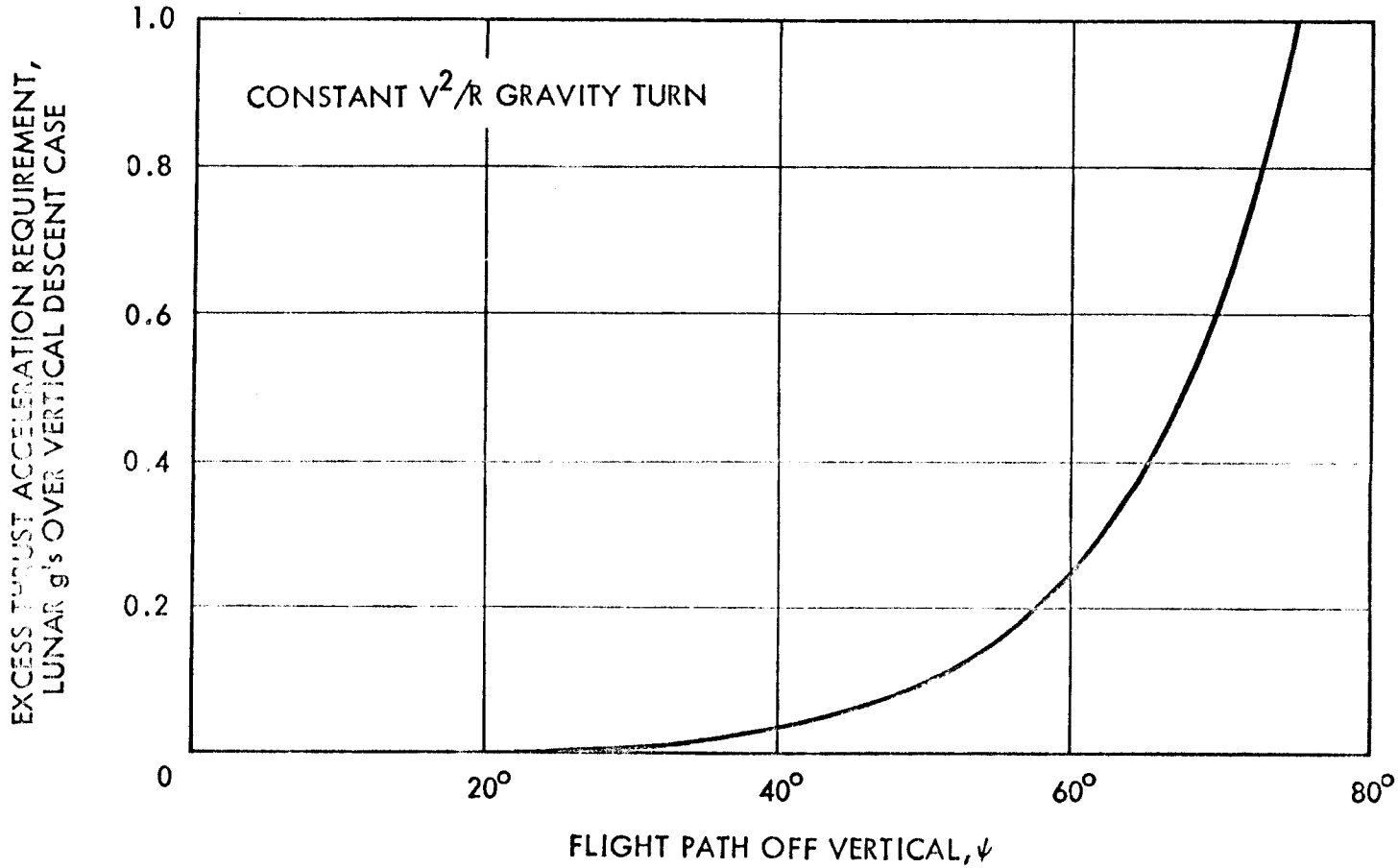


FIGURE 11. EXCESS THRUST ACCELERATION REQUIREMENT OVER VERTICAL DESCENT

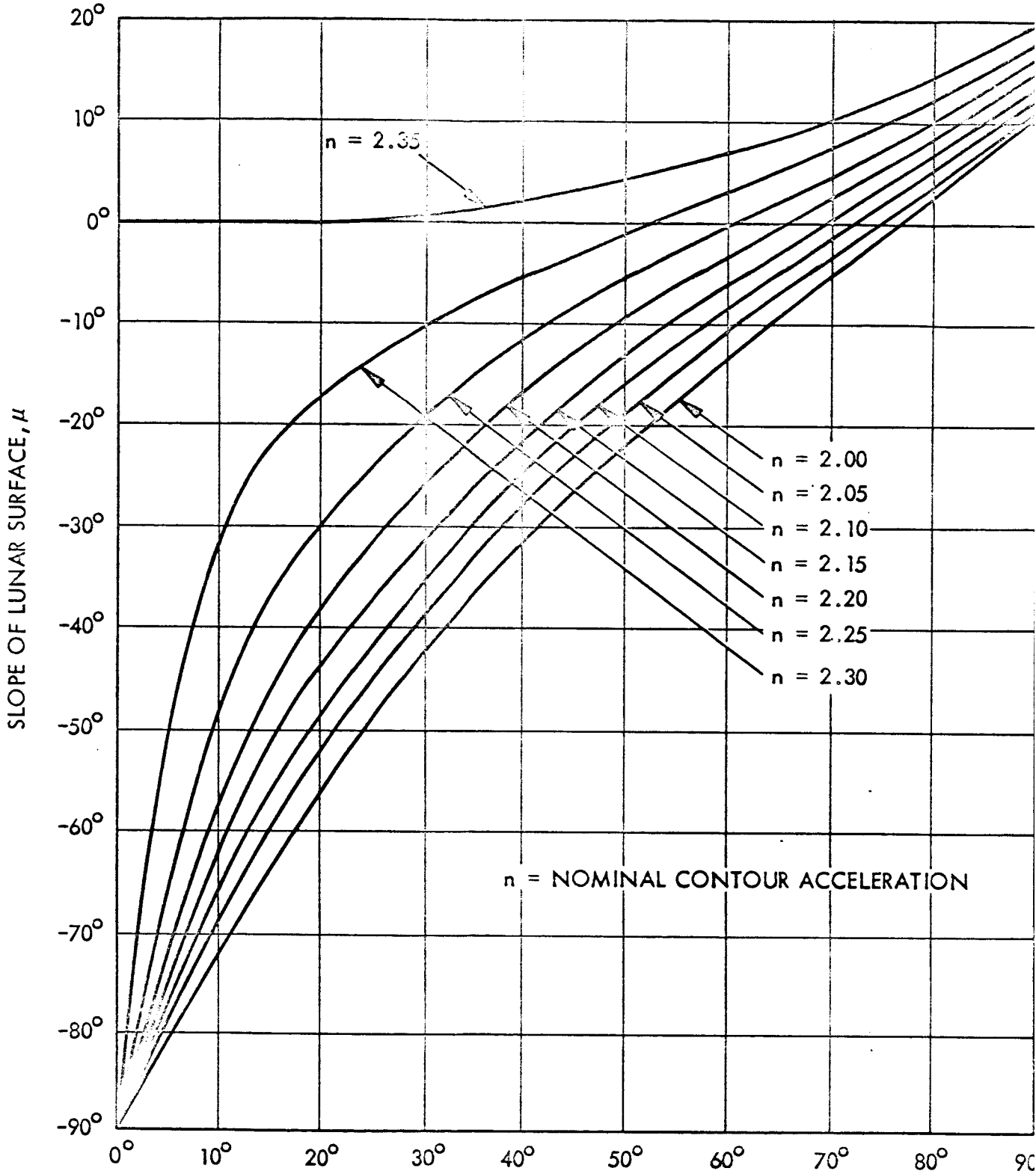


FIGURE 12. SLOPE-FLIGHT PATH CAPABILITY VERSUS NOMINAL CONTOUR ACCELERATION LEVEL FOR 2.35 g ACCELERATION LIMIT ($n_{max}$ = 2.35)

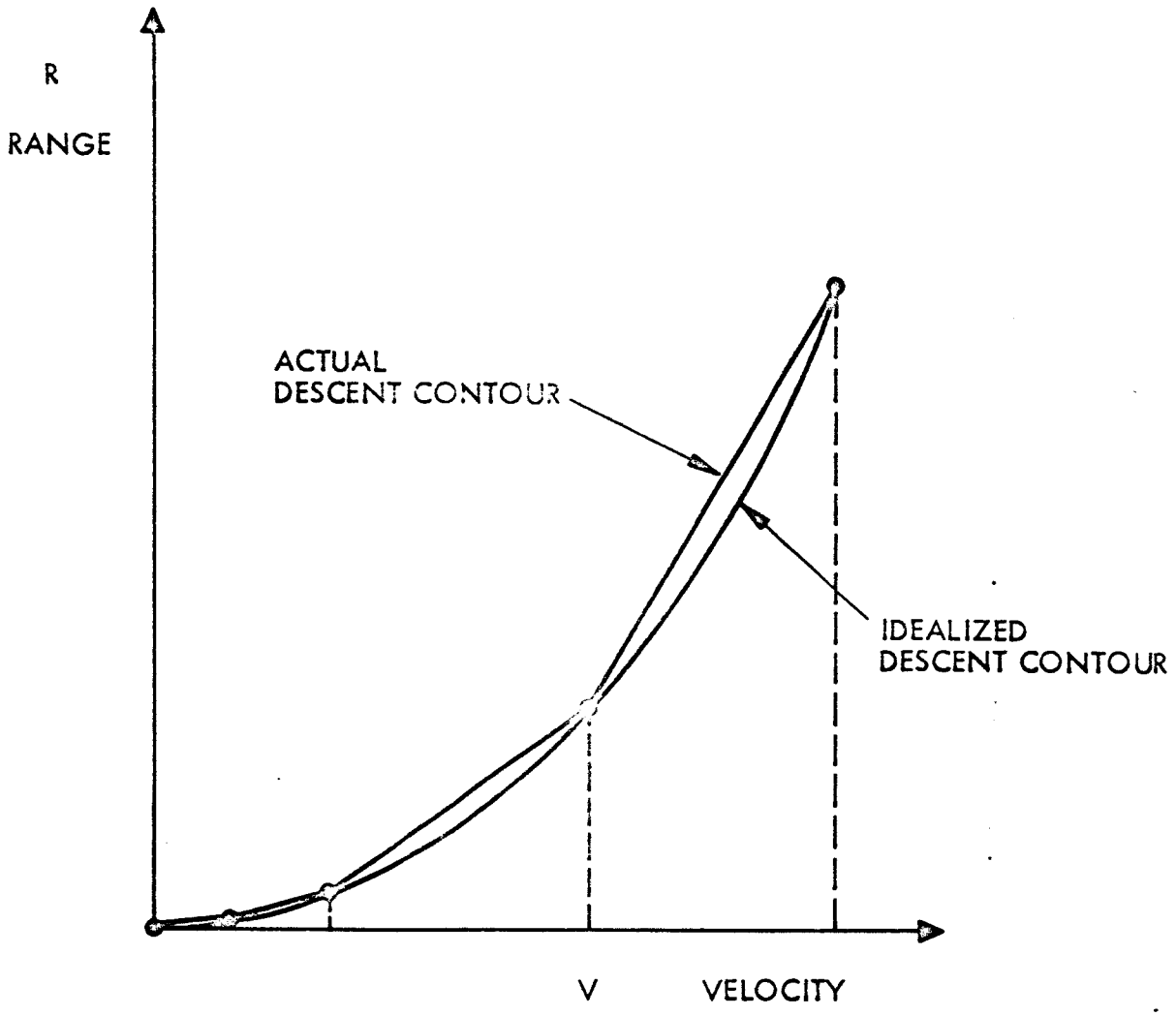


FIGURE 13. 4-SEGMENT APPROXIMATION OF PARABOLIC DESCENT CONTOUR

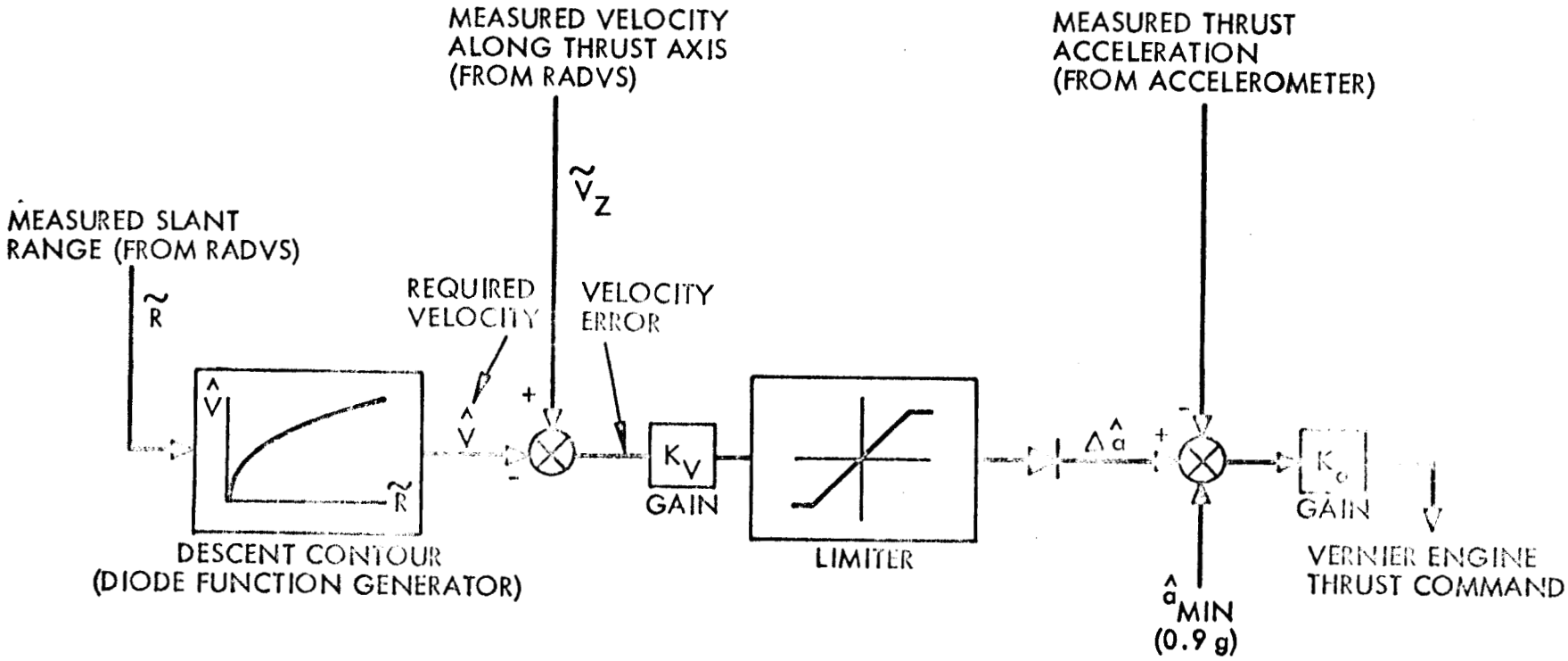


FIGURE 14. THRUST ACCELERATION COMMAND MECHANIZATION

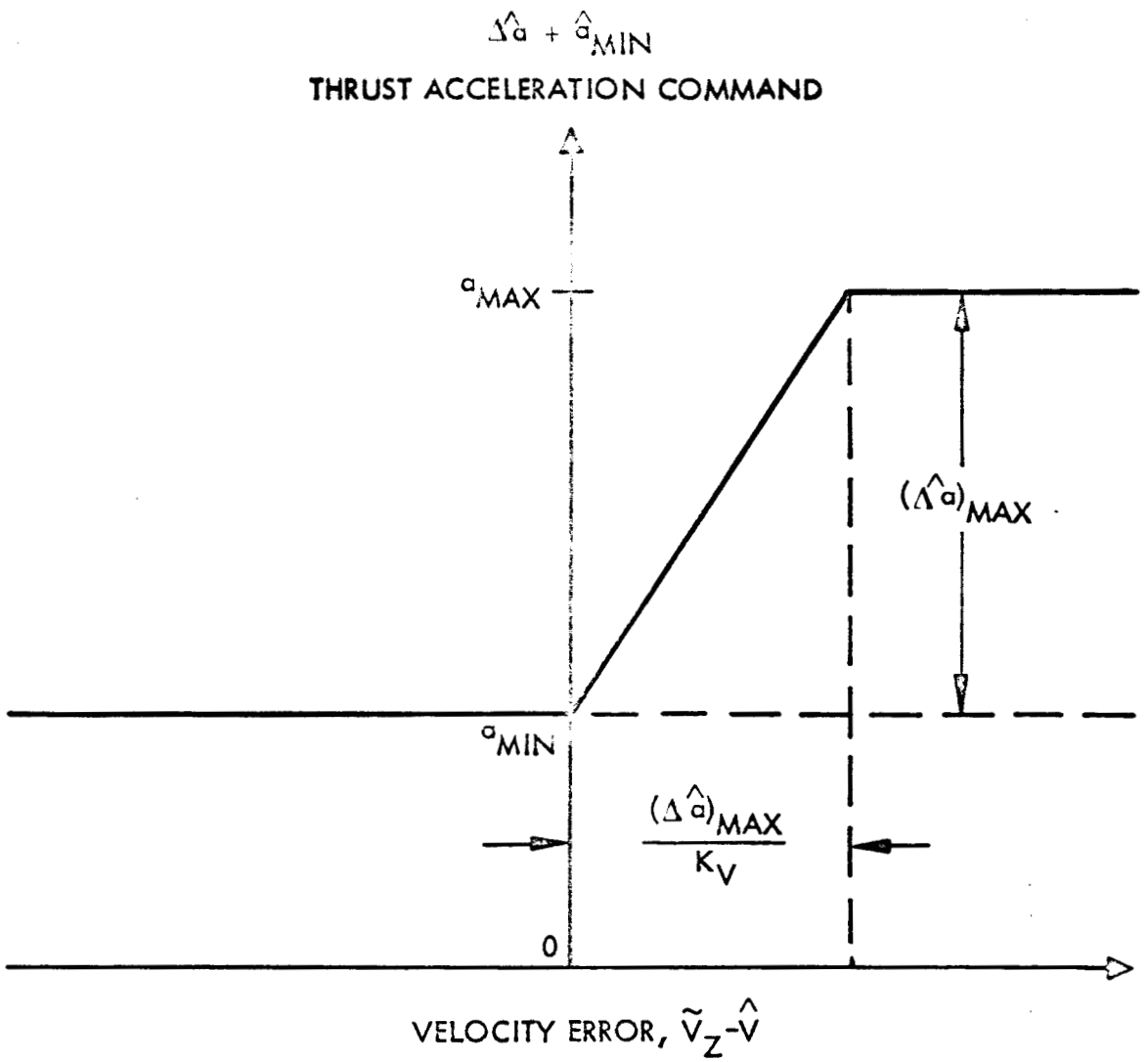


FIGURE 15. THRUST ACCELERATION COMMAND CHARACTERISTIC

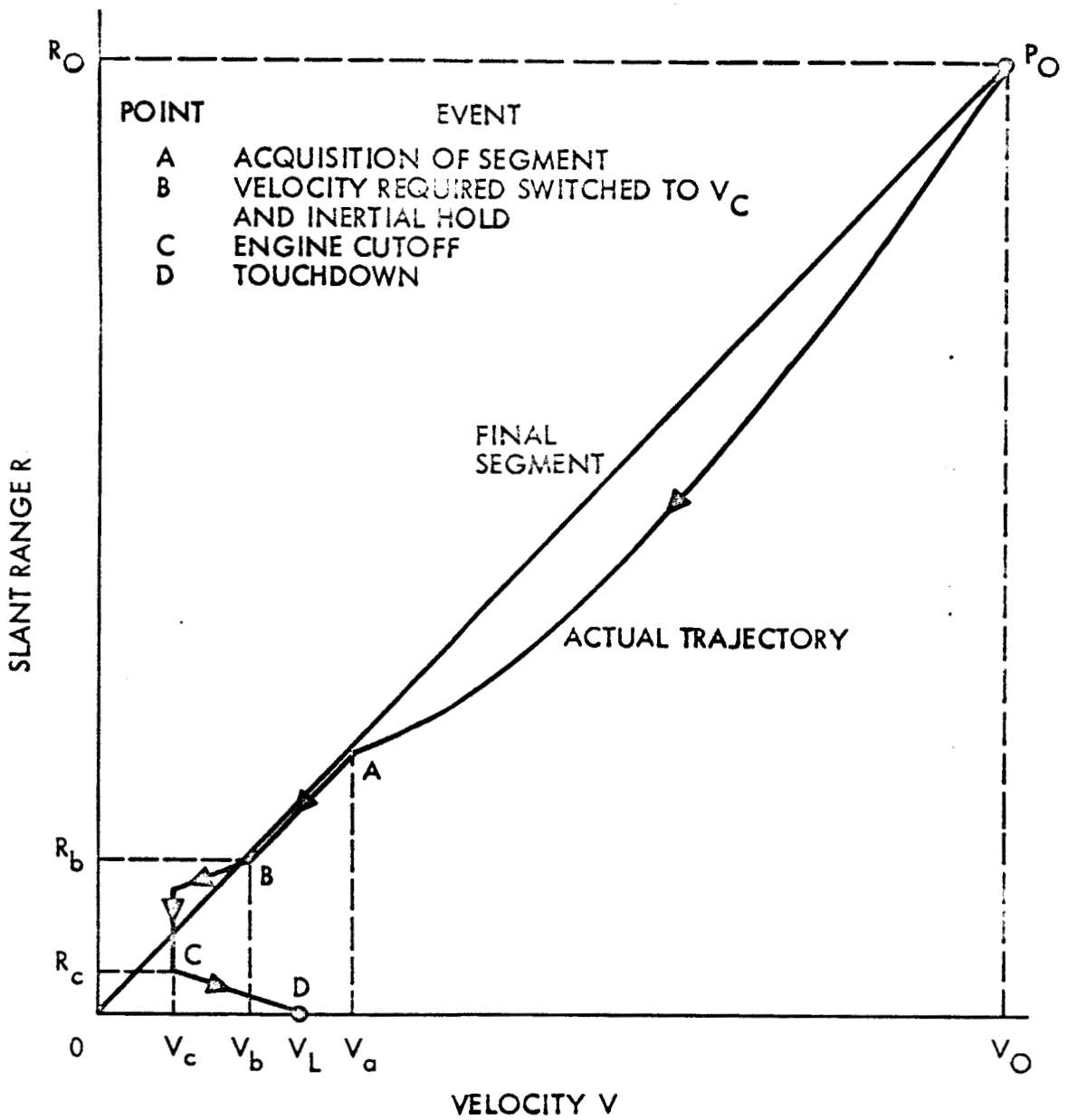


FIGURE 16. TRAJECTORY ALONG FINAL SEGMENT